Biofabrication

DOI: 10.1002/anie.201409846

Biofabrication of Cell-Loaded 3D Spider Silk Constructs**

Kristin Schacht, Tomasz Jüngst, Matthias Schweinlin, Andrea Ewald, Jürgen Groll, and Thomas Scheibel**

Abstract: *Biofabrication is an emerging and rapidly expanding field of research in which additive manufacturing techniques in combination with cell printing are exploited to generate hierarchical tissue-like structures. Materials that combine printability with cytocompatibility, so called bioinks, are currently the biggest bottleneck. Since recombinant spider silk proteins are non-immunogenic, cytocompatible, and exhibit physical crosslinking, their potential as a new bioink system was evaluated. Cell-loaded spider silk constructs can be printed by robotic dispensing without the need for crosslinking additives or thickeners for mechanical stabilization. Cells are able to adhere and proliferate with good viability over at least one week in such spider silk scaffolds. Introduction of a cell-binding motif to the spider silk protein further enables fine-tuned control over cell–material interactions. Spider silk hydrogels are thus a highly attractive novel bioink for biofabrication.*

Research in tissue engineering is traditionally focused on the seeding of cells into porous material scaffolds in order to generate a three-dimensional (3D) cell–material construct. By using biodegradable materials with optimized scaffold porosity, generated for example by additive manufacturing (AM) techniques, promising results have been achieved in the context of the repair and/or regeneration of tissues.[1] One current focus of research is on seeding and culturing various cell types in 3D environments that closely mimic the native extracellular matrix (ECM).[2] This is based on the fact that scaffolds must support cellular adhesion, growth, proliferation, migration, and, in case of progenitor cells, differentiation.[3] Recently, a rapidly growing number of studies have focused on biomimicry beyond the ECM and the generation of cell-loaded tissue-like hierarchical structures.[4] To achieve this goal, it is important to choose materials with properties and functions which mimic the tissue that needs to be replaced on the macroscopic scale.[5] Moreover, such morphologies cannot be reached by seeding cells on prefabricated scaffolds; they are only achievable through the combined 3D printing of cells and materials.

In addition to cytocompatibility, the printed materials (so called "bioinks") must show distinct physicochemical properties. For example, they should exhibit viscous fluid behavior within the printing head but polymerize shortly after extrusion. In contrast to other AM techniques, robotic dispensing enables the printing of clinically relevant scaffolds containing biologically active substances and even cells. This technique also allows the simultaneous processing of multiple materials, which enables reproduction of the zonal structures of tissues.[6] However, only few materials have so far been developed for this purpose, with hydrogels as the most promising candidates.[7] Hydrogels are well established for applications in tissue regeneration.[8] They are usually based on a variety of synthetically derived polymers, such as poly(acrylic acid) (PAA), poly(ethylenglycol) (PEG), and poly-(ethylene oxide) (PEO), as well as naturally derived polymers such as agarose, alginate, chitosan, collagen, or silk.[8a,9] Concerning silk, in previous works, an inkjet printing process was developed for the fabrication of microscopic arrays of silkworm silk "nests" capable of hosting live cells for prospective biosensors.[10] Spider silk materials are particularly interesting for biomedical use since they show an absence of toxicity, slow degradation, little or no immunogenicity, wide pore-size distribution, and elastic properties.[11] Hydrogels made of recombinant spider silk proteins are physically crosslinked by β-sheet structures, hydrophobic interactions, and entanglement. The morphology and pore sizes of spider silk hydrogels depend on protein concentration and can be further influenced through functionalization of the protein.[12]

In this study, hydrogels of recombinant spider silk proteins were produced and used as a new bioink for the automatized generation of 3D cell-loaded constructs. The recombinant spider silk protein eADF4(C16) and a variant containing an RGD motif were applied and assessed with regard to their printability, the possibility to encapsulate cells, and finally the generation of cell-loaded 3D hydrogel constructs through the printing of cells suspended in spider silk protein solutions.[13]

[*] K. Schacht,[+] Prof. Dr. T. Scheibel
Lehrstuhl Biomaterialien, Universität Bayreuth
Universitätsstraße 30, 95447 Bayreuth (Germany)
E-mail: thomas.scheibel@bm.uni-bayreuth.de
T. Jüngst,[+] Dr. A. Ewald, Prof. Dr. J. Groll
Lehrstuhl für Funktionswerkstoffe der Medizin
und der Zahnheilkunde, Universitätsklinikum Würzburg
Pleicherwall 2, 97070 Würzburg (Germany)
E-mail: juergen.groll@fmz.uni-wuerzburg.de
M. Schweinlin
Lehrstuhl für Tissue Engineering und Regenerative Medizin
Universitätsklinikum Würzburg
Röntgenring 11, 97070 Würzburg (Germany)
[+] These authors contributed equally to this work.

[**] We would like to thank Andreas Schmidt for fermentation and purification of the proteins; Martin Humenik, Kathrin Hahn, Simone Werner, Florian Gisdon, and Jan Scheler for experimental help; Stefanie Wohlrab, Elise DeSimone, Kiran Pawar, Martina Elsner, and Martin Humenik for proof reading and discussions; and Joschka Bauer for discussions and technical support in creating the artwork. Funding was obtained from the DFG (SCHE 603/9-1) and the European Union's Seventh Framework Programm (FP7/2007-2013) under grant agreement no. 309962 (project HydroZones).

Supporting information for this article is available on the WWW under http://dx.doi.org/10.1002/anie.201409846.

Like most concentrated polymer networks, hydrogels made of spider silk proteins demonstrate viscoelastic behavior, with stress changes proportional to linearly increasing strain (Figure S1 in the Supporting Information).[14] The elastic modulus of the eADF4(C16) hydrogel (3 % w/v) was approximately 0.02 kPa, and that of the eADF4(C16)-RGD hydrogel (3 % w/v) was approximately 0.2 kPa, which is in the range of soft human tissues and organs.[11] Shear thinning of the gels was analyzed through oscillating measurements with an oscillating stress of 10 Pa (Figure S2). The storage moduli (G′) exceeded the loss moduli (G″) over the whole angular frequency range, and both moduli were slightly dependent on frequency. In these hydrogels, elastic behavior dominates over viscous behavior, with low-viscosity flow behavior and good form stability. Additionally, eADF4 hydrogels showed shear-thinning (non-Newtonian) behavior, with high viscosity at low angular frequencies and a decrease in viscosity at higher frequencies (Figure S2B).

One important feature of hydrogels as cell scaffolds is sufficient diffusion of nutrients, oxygen, and waste products during cultivation. 5(6)-carboxyfluorescein or fluorescein isothiocyanate (FITC)-conjugated dextrans were used as model compounds for diffusion. It was shown that the transport of nutrients and waste products through both eADF4(C16) and eADF4(C16)-RGD hydrogels is possible, even for the high-molecular-weight FITC-dextran (500 kDa), although its diffusion was limited (Figure S2C,D).

To evaluate general cytocompatibility, cell adhesion of BALB/3T3 mouse fibroblasts to the eADF4(C16) and eADF4(C16)-RGD hydrogels was tested. The cell adhesion of mouse fibroblasts was weak on eADF4(C16) hydrogels, as shown by a round shape and cell aggregation (Figure 1 A,B,E). Owing to the lack of cell adhesion motifs in eADF4(C16), adhesion is mostly influenced by surface charge, as well as the hydrophobicity and topography of the scaffold.[13c,15] On eADF4(C16)-RGD hydrogels, mouse fibroblasts were well spread and showed filopodia, a result consistent with previous observations of mouse fibroblasts growing on films and non-woven meshes made of eADF4-(C16)-RGD (Figure 1 C).[13c,15a] For all of the tested cell lines (fibroblasts, myoblasts, HeLa cells, osteoblasts, and keratinocytes), cell adhesion on eADF4(C16)-RGD hydrogels was significantly improved in comparison to unmodified eADF4-(C16) hydrogels (Figure 1).

Interestingly, the adhesion of osteoblasts is much better on eADF4(C16) hydrogels compared to the other cell lines. This osteoblast-specific phenomenon is not yet fully understood. In addition to improved adhesion, the proliferation of fibroblasts was better on eADF4(C16)-RGD hydrogels in comparison to eADF4(C16) hydrogels. Based on these findings, eADF4 hydrogels were printed by using robotic dispensing (Figure 2 A). Initial attempts to print with a printhead that dispenses material based on a time–pressure principle failed owing to inconsistent filament diameter. Ultimately, we used a printhead with an electromagnetic valve in combination with a 0.3 mm nozzle to print meshes with a filament center-to-center distance of 2 mm. With this printhead, the hydrogels were process compatible and had high shape fidelity, based on the β-sheet transformation during gelation and the shear thinning behavior (Table S1, Figure S2A,B). The ultrastructural integrity was also evaluated. It was possible to print up to 16 layers on top of each other with a construct depth of approximately 3 mm without structural collapse (Figure 2 B–D and Figure S3).

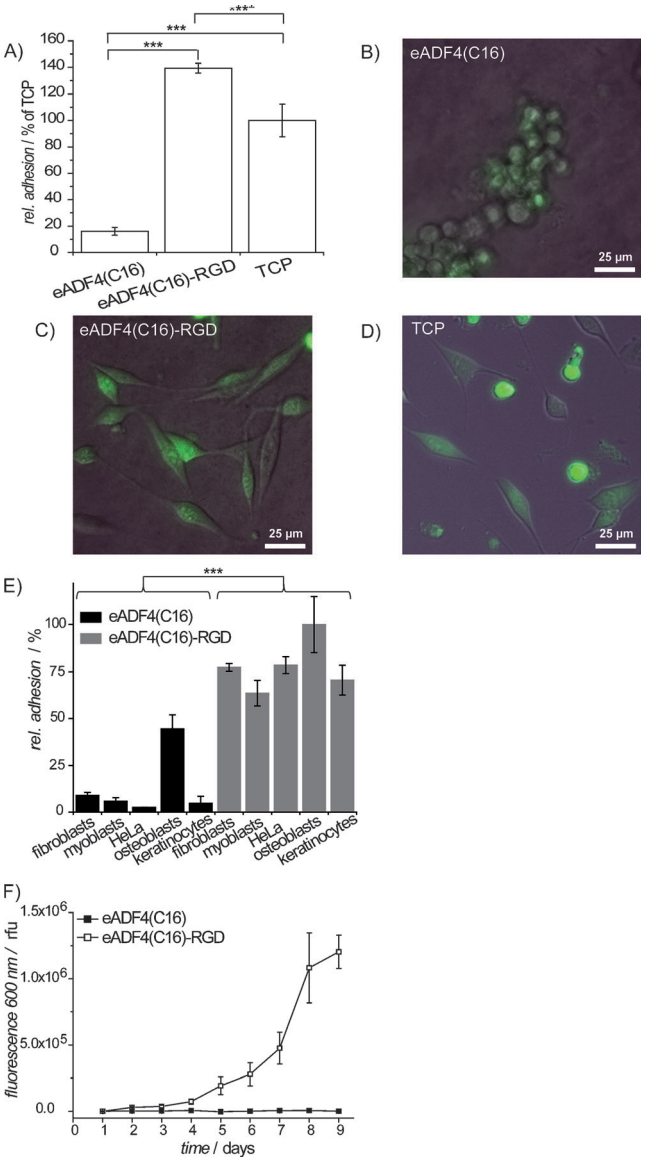

Figure 1. Cultivation of different cell lines on hydrogels made of 3 % eADF4(C16) or 3 % eADF4(C16)-RGD. A) BALB/3T3 fibroblast adhesion was quantified by using the cell-titer blue assay and normalized to adhesion onto treated tissue culture plates (TCP) as the 100 % value. The adhesion of fibroblasts was significantly (***$p < 0.001$) higher on eADF4(C16)-RGD hydrogels than eADF4(C16) hydrogels and TCP. B–D) Live-cell microscopy of BALB/3T3 mouse fibroblasts cultivated on eADF4(C16) (B) and eADF4(C16)-RGD (C) hydrogels and treated tissue culture plates (D) after 24 h of incubation. The cells were stained with the Vybrant CFDA SE Cell Tracer Kit. Scale bars: 50 µm. E) Adhesion of different cell lines to respective hydrogels. Adhesion of osteoblasts to eADF4(C16)-RGD hydrogels was set to 100 %. The adhesion of all of the tested cell lines was significantly improved (***$p < 0.001$) on eADF4(C16)-RGD hydrogels compared to eADF4(C16) hydrogels. F) Proliferation of fibroblasts was quantified by using the cell-titer blue assay.

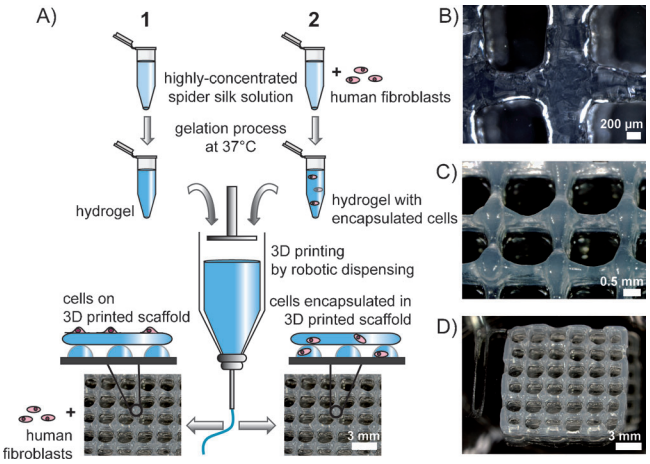

Figure 2. 3D printing of spider silk scaffolds by robotic dispensing. A) Schematic representation of 3D-printing. Cells were either cultivated on the 3D-scaffold (1) or encapsulated during processing (2). Stereomicroscopy and digital images of 2-layer eADF4(C16) (B) and 8-layer eADF4(C16) scaffolds (C, D) are shown.

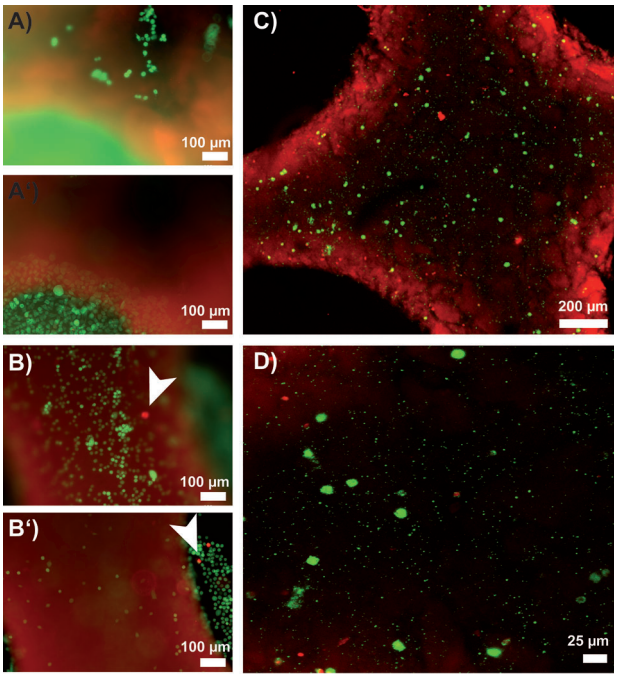

Figure 3. Human fibroblasts cultivated on printed 2-layer eADF4(C16) (A) and eADF4(C16)-RGD (B) hydrogels after 24 h of incubation. Fluorescence microscopy images of cells stained with calcein A/M (live cells: green) and ethidium homodimer I (dead cells; red). Ethidium homodimer I also stained the printed scaffolds. A, B) Focus on the hydrogel. A′, B′) Focus on the well-plate. White arrow: dead cells. (The corresponding confocal laser scanning microscopy images are included in Figure S4A,B). C, D) Confocal laser scanning microscopy images of human fibroblasts encapsulated in a printed 2-layer eADF4(C16) hydrogel after 48 h of incubation (corresponding fluorescence microscopy images are included in Figure S4C–F).

In a first approach, human fibroblasts were seeded on the scaffolds directly after printing. Human fibroblasts adhered weakly on the surface of printed eADF4(C16) hydrogels after 24 h, while the cells spread on scaffolds made of eADF4-(C16)-RGD (Figure 3 and Figure S4A,B). These results correlate well with the experiments performed on the respective hydrogels prepared conventionally and indicate that robotic dispensing does not negatively alter the cell–material interactions of the spider silk proteins. No structural changes occur during the printing process and the shear stress during printing does not influence the cell behavior (Table S1).

Given these results, the next step was to mix human fibroblasts with highly concentrated 3% w/v eADF4(C16) silk solution before gelation in an incubator at 37°C. The addition of cells to the bioink did not influence the printability of the material. The printing parameters only needed minor modifications compared to cell-free inks: an increase of the barrel pressure from 1.0 bar to 1.1 bar and a delay of the valve opening time from 700 microseconds to 900 microseconds. All other parameters could be kept constant without reducing printing fidelity. Cell viability was evaluated at 24, 48, 72 h, and 7 days after printing by live/dead staining. It was confirmed that, when encapsulated in eADF4(C16) hydrogels, the human fibroblasts survived the printing process and were viable for at least seven days in situ, even in the absence of cell adhesion domains (Figure 3 C,D and Figure S4C–F). We quantified viability according to the live/dead assays and detected an average viability of $70.1 \pm 7.6\%$ after 48 h of incubation. However, in this context it is important to note that reference samples with cells incubated in the spider silk hydrogels without printing showed almost identical survival rates, so that the relative survival rate of cells in printed versus non printed gels is 97%. Hence, although cell viability in the spider silk constructs is lower when compared to established bioinks such as alginate (usually 90%) and gelatin (usually 98%), we could show that the printing procedure does not affect viability.[16] Most importantly, and in contrast to the mentioned established systems, our spider silk offers the possibility to biotechnologically and thus precisely tune the biochemical properties in terms of cell adhesion and proliferation, which will in future studies be performed and optimized for printing. Given these results, as well the the low batch-to-batch variations of the material and high reproducibility of the printing, we are confident that recombinant spider silk can be established as a bioink system for biofabrication. The cells were spherical in shape and were homogeneously distributed within the constructs. Cell density did not seem to differ between the constructs, thus leading to the conclusion that cells were distributed homogeneously within the syringe and no sedimentation occurred during gelation. The cells were spherical in shape because movement of the cells was hindered by the dense nanofibrillar matrix. Cellular mobility can be dependent on microenvironmental conditions, such as morphology, space, substrate stiffness, and hydrophobicity.[17] Accordingly, the spherical shape was also detected for primary dermal fibroblasts encapsulated in alginate or fibrin hydrogels.[18]

In conclusion, it could be demonstrated that recombinant spider silk proteins can be used as bioink for 3D printing without the need for additional components or post-processing. By contrast, alginate, which is one of the most frequently

used bioinks for 3D printing, shows less pronounced shear thinning behavior than the silk used in this study. Therefore, post-processing with a crosslinker (calcium ions) or the addition of thickeners is necessary to increase the printing fidelity of alginate, whereas the recombinant spider silk hydrogels can be printed without additives or additional crosslinking.[19] In the case of recombinant spider silk proteins, cells can be directly added to the printing solution, thus resulting in 3D printed cell-loaded constructs with high cell viability for at least seven days. The introduction of a cell-adhesion motif in the spider silk protein also enables control over the cell–material interactions. This is thus a powerful new system that significantly broadens the material spectrum within the field of biofabrication.

Experimental Section

Hydrogel preparation: The recombinant spider silk protein eADF4-(C16) consists of 16 repeats of module C (sequence: GSSAAAAAAAASGPGGYG PENQGPSGPGGYGPGGP), which mimics the repetitive core sequence of dragline silk fibroin 4 (ADF4) of the European garden spider *Araneus diadematus*.[13a,b] eADF4(C16) (MW: 47698 g mol^{-1}) and eADF4(C16)-RGD (MW: 48583 g mol^{-1}) were produced and purified as described previously.[13a,c] 30 mg mL^{-1} (3% w/v) eADF4(C16) and eADF4(C16)-RGD solutions were prepared as described previously[12e] (see the Supporting Information). Gels were formed overnight at 37°C and 95% relative humidity.[12e] Recombinant spider silk protein eADF4(C16) and its variants can be produced under good manufacturing practice (GMP) conditions and printing was performed in a biosafety cabinet in a cell culture laboratory, with sterile conditions and media. For the in vitro assays performed in this study, no further additional sterilization was performed and we did not encounter any problems with contamination. Nevertheless, for further long term studies and in vivo investigations, sterilization methods (e.g., autoclaving, sterile filtration, or γ-irradiation) have already been developed for the recombinant spider silks.[20]

Cell culture experiments: For details of the cell lines and their cultivation and preparation before the experiments, see the Supporting Information. For all cell culture experiments, hydrogels were washed twice with cell culture medium before seeding the cells. For cell morphology analysis, BALB/3T3 mouse fibroblasts were seeded on eADF4(C16) and eADF4(C16)-RGD hydrogels with an initial cell density of 47000 cells cm^{-2}. As a positive control, the (well-adhering) cells were seeded on commercially available treated tissue culture plates (TCP; Nunc). Cells were stained with carboxyfluorescein diacetate succinimidyl ester [Vybrant CFDA SE Cell Tracer Kit (Life Technologies GmbH)], and after 24 h of incubation they were visualized with a live-cell microscope (Leica). For cell adhesion tests, 3% w/v eADF4(C16) and 3% w/v eADF4(C16)-RGD solutions were placed in Millicell inserts with 8 μm pore diameter, and the hydrogels were formed overnight at 37°C. The next day, 75000 cells cm^{-2} were seeded on the hydrogels for 2.5 h. After cultivation, the hydrogels were washed twice with phosphate-buffered saline (PBS; Sigma Aldrich) to remove non-attached or dead cells, followed by the addition of fresh medium. After incubation for 4 h with 10% v/v CellTiter-Blue reagent (Promega), cell adhesion was quantified by determining the fluorescence intensity of resorufin (λ_{ex} 530 nm; λ_{em} 590 nm) by using a plate reader (Mithras LB 940). All cell adhesion experiments were repeated three times with three replicates each time. The statistical analyses were performed with the software package STATISTICA 12.0 (StatSoft Inc). An independent Student's *t*-test (two-tailed) was performed on the absolute values of the adhesion tests. Prior to the *t*-test, the homogeneity of variances was tested with Levene's test. The sample variances were considered equal if the *p*-value of the Levene's test was greater than 0.05. For cell proliferation analysis, 5000 cells cm^{-2} were cultivated on eADF4-(C16) and eADF4(C16)-RGD hydrogels for 9 days. Once every 24 h, the samples were washed with PBS and the cells quantified by using the CellTiter-Blue assay. The samples were then washed twice with medium and incubated in fresh medium under controlled atmosphere until the next day. The proliferation experiments were repeated twice with three replicates per experiment. For analysis of the printed 2-layer eADF4(C16) and eADF4(C16)-RGD scaffolds, human fibroblasts were cultivated on the scaffolds with a cell seeding density of 75000 cells cm^{-2}. Cells and scaffolds were stained with Calcein acetoxymethyl ester (Calcein A/M) and Ethidium Homodimer I (Invitrogen; see the Supporting Information). Live and dead cells, as well as the scaffolds, were visualized with a fluorescence microscope (Carl Zeiss Axio Observer.Z1) and a confocal scanning microscope (Leica TCS SP8 STED). Confocal laser scanning microscopy images of human fibroblasts encapsulated in a printed 2-layer eADF4(C16) hydrogel were made at a cell density of 1200000 cells mL^{-1} after 48 h of incubation.

3D printing through robotic dispensing: Robotic dispensing was performed by using a Bioplotter (regenHU) in a laminar-flow hood. The printhead (CF-300N/H cell-friendly printhead for contact dispensing) operated in the *y*,*z* plane and the collector along the *x* axis. Before printing, the spider silk solutions were pre-gelled overnight at 37°C and 95% relative humidity (Figure 2A).[12e] During printing, the material was stored at room temperature in a pressurized 3cc syringe (Nordson EFD). Precise dispensing was achieved by using an electromagnetic valve positioned in front of a nozzle with an inner diameter of 0.3 mm, with a resulting strand width of 626 ± 8 μm. The valve opening time was 700–900 μs and the flow was regulated by pressure (1.0–1.1 bar). The printed constructs were analyzed with a stereomicroscope (Carl Zeiss SteREO Discovery.V20).

Received: October 7, 2014
Revised: November 21, 2014
Published online: January 13, 2015

Keywords: biofabrication · cell encapsulation · fibroblasts · hydrogels · spider silk

[1] S. J. Hollister, *Nat. Mater.* **2005**, *4*, 518–524.
[2] a) X. Q. Jia, K. L. Kiick, *Macromol. Biosci.* **2009**, *9*, 140–156; b) V. A. Schulte, K. Hahn, A. Dhanasingh, K. H. Heffels, J. Groll, *Biofabrication* **2014**, *6*, 024106.
[3] a) M. P. Lutolf, J. A. Hubbell, *Nat. Biotechnol.* **2005**, *23*, 47–55; b) A. J. Engler, S. Sen, H. L. Sweeney, D. E. Discher, *Cell* **2006**, *126*, 677–689; c) A. J. Engler, P. O. Humbert, B. Wehrle-Haller, V. M. Weaver, *Science* **2009**, *324*, 208–212; d) P. J. Reddig, R. L. Juliano, *Cancer Metastasis Rev.* **2005**, *24*, 425–439.
[4] B. Derby, *Science* **2012**, *338*, 921–926.
[5] a) J. H. Shim, S. E. Kim, J. Y. Park, J. Kundu, S. W. Kim, S. S. Kang, D. W. Cho, *Tissue Eng. Part A* **2014**, *20*, 1980–1992; b) B. Duan, L. A. Hockaday, K. H. Kang, J. T. Butcher, *J. Biomed. Mater. Res. Part A* **2012**, *101*, 1255–1264; c) F. P. W. Melchels, W. J. A. Dhert, D. W. Hutmacher, J. Malda, *J. Mater. Chem. B* **2014**, *2*, 2282–2289.
[6] a) W. Schuurman, P. A. Levett, M. W. Pot, P. R. van Weeren, W. J. A. Dhert, D. W. Hutmacher, F. P. W. Melchels, T. J. Klein, J. Malda, *Macromol. Biosci.* **2013**, *13*, 551–561; b) P. Bajaj, R. M. Schweller, A. Khademhosseini, J. L. West, R. Bashir, *Annu. Rev. Biomed. Eng.* **2014**, *16*, 247–276; c) W. Schuurman, V. Khristov, M. W. Pot, P. R. van Weeren, W. J. A. Dhert, J. Malda, *Biofabrication* **2011**, *3*, 021001.
[7] J. Malda, J. Visser, F. P. Melchels, T. Jungst, W. E. Hennink, W. J. A. Dhert, J. Groll, D. W. Hutmacher, *Adv. Mater.* **2013**, *25*, 5011–5028.

[8] a) J. L. Drury, D. J. Mooney, *Biomaterials* **2003**, *24*, 4337 – 4351; b) M. W. Tibbitt, K. S. Anseth, *Biotechnol. Bioeng.* **2009**, *103*, 655 – 663; c) O. Wichterle, D. Lim, *Nature* **1960**, *185*, 117 – 118; d) K. R. Kamath, K. Park, *Adv. Drug Delivery Rev.* **1993**, *11*, 59 – 84.

[9] a) I. Armentano, M. Dottori, E. Fortunati, S. Mattioli, J. M. Kenny, *Polym. Degrad. Stab.* **2010**, *95*, 2126 – 2146; b) K. Y. Lee, D. J. Mooney, *Chem. Rev.* **2001**, *101*, 1869 – 1879.

[10] R. Suntivich, I. Drachuk, R. Calabrese, D. L. Kaplan, V. V. Tsukruk, *Biomacromolecules* **2014**, *15*, 1428 – 1435.

[11] A. Leal-Egaña, T. Scheibel, *Biotechnol. Appl. Biochem.* **2010**, *55*, 155 – 167.

[12] a) S. Rammensee, D. Huemmerich, K. D. Hermanson, T. Scheibel, A. R. Bausch, *Appl. Phys. A* **2006**, *82*, 261 – 264; b) U. J. Kim, J. Y. Park, C. M. Li, H. J. Jin, R. Valluzzi, D. L. Kaplan, *Biomacromolecules* **2004**, *5*, 786 – 792; c) A. Matsumoto, J. Chen, A. L. Collette, U. J. Kim, G. H. Altman, P. Cebe, D. L. Kaplan, *J. Phys. Chem. B* **2006**, *110*, 21630 – 21638; d) X. Q. Wang, J. A. Kluge, G. G. Leisk, D. L. Kaplan, *Biomaterials* **2008**, *29*, 1054 – 1064; e) K. Schacht, T. Scheibel, *Biomacromolecules* **2011**, *12*, 2488 – 2495.

[13] a) D. Huemmerich, C. W. Helsen, S. Quedzuweit, J. Oschmann, R. Rudolph, T. Scheibel, *Biochemistry* **2004**, *43*, 13604 – 13612; b) C. Vendrely, T. Scheibel, *Macromol. Biosci.* **2007**, *7*, 401 – 409; c) S. Wohlrab, S. Muller, A. Schmidt, S. Neubauer, H. Kessler, A. Leal-Egaña, T. Scheibel, *Biomaterials* **2012**, *33*, 6650 – 6659.

[14] F. C. Mackintosh, J. Kas, P. A. Janmey, *Phys. Rev. Lett.* **1995**, *75*, 4425 – 4428.

[15] a) A. Leal-Egaña, G. Lang, C. Mauerer, J. Wickinghoff, M. Weber, S. Geimer, T. Scheibel, *Adv. Eng. Mater.* **2012**, *14*, B67 – B75; b) F. Bauer, S. Wohlrab, T. Scheibel, *Biomater. Sci.* **2013**, *1*, 1244 – 1249.

[16] a) J. Jia, D. J. Richards, S. Pollard, Y. Tan, J. Rodriguez, R. P. Visconti, T. C. Trusk, M. J. Yost, H. Yao, R. R. Markwald, Y. Mei, *Acta Biomater.* **2014**, *10*, 4323 – 4331; b) T. Billiet, E. Gevaert, T. De Schryver, M. Cornelissen, P. Dubruel, *Biomaterials* **2014**, *35*, 49 – 62.

[17] a) L. Moroni, L. P. Lee, *J. Biomed. Mater. Res. A* **2009**, *88A*, 644 – 653; b) B. M. Gillette, J. A. Jensen, B. X. Tang, G. J. Yang, A. Bazargan-Lari, M. Zhong, S. K. Sia, *Nat. Mater.* **2008**, *7*, 636 – 640; c) T. Yeung, P. C. Georges, L. A. Flanagan, B. Marg, M. Ortiz, M. Funaki, N. Zahir, W. Y. Ming, V. Weaver, P. A. Janmey, *Cell Motil. Cytoskeleton* **2005**, *60*, 24 – 34; d) J. C. M. Teo, R. R. G. Ng, C. P. Ng, A. W. H. Lin, *Acta Biomater.* **2011**, *7*, 2060 – 2069.

[18] C. M. Hwang, B. Ay, D. L. Kaplan, J. P. Rubin, K. G. Marra, A. Atala, J. J. Yoo, S. J. Lee, *Biomed. Mater.* **2013**, *8*, 014105.

[19] S. Wüst, M. E. Godla, R. Muller, S. Hofmann, *Acta Biomater.* **2014**, *10*, 630 – 640.

[20] a) D. N. Rockwood, R. C. Preda, T. Yucel, X. Q. Wang, M. L. Lovett, D. L. Kaplan, *Nat. Protoc.* **2011**, *6*, 1612 – 1631; b) E. S. Gil, S. H. Park, X. Hu, P. Cebe, D. L. Kaplan, *Macromol. Biosci.* **2014**, *14*, 257 – 269.

